

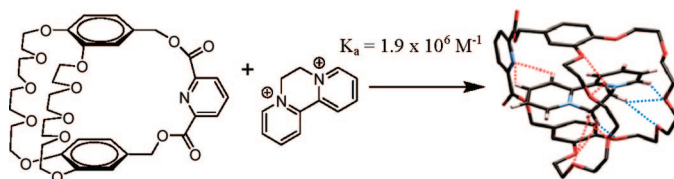
High-Yielding, Regiospecific Synthesis of *cis*(4,4′)-Di(carbomethoxybenzo)-30-crown-10, Its Conversion to a Pyridyl Cryptand and Strong Complexation of 2,2′- and 4,4′-Bipyridinium Derivatives

Adam M.-P. Pederson, Elizabeth M. Ward, Daniel V. Schoonover, Carla Slebodnick, and Harry W. Gibson*

Department of Chemistry, Virginia Polytechnic Institute and State University,
Blacksburg, Virginia 24061-0212

hwgibson@vt.edu

Received August 25, 2008



A high yielding (93%), regiospecific synthesis of *cis*(4,4′)-di(carbomethoxybenzo)-30-crown-10 (**1c**) is reported. The derived crown ether diol **1d** was converted to pyridyl cryptand **12** in 44% yield by reaction with pyridine-2,6-dicarbonyl chloride. Binding of two different 4,4′-bipyridinium (paraquat) species (**3**) and 2,2′-bipyridinium (diquat) **4** by **12** was explored via ¹H NMR spectroscopy, NOE experiments, mass spectrometry, X-ray crystallographic analyses, and isothermal titration calorimetry. Cryptand **12** exhibits the highest association constant for diquat ever reported ($K_a = 1.9 \times 10^6 \text{ M}^{-1}$) and very high association constants for paraquats ($K_a > 10^5 \text{ M}^{-1}$) in acetone at 22 °C. The binding constant of diquat **4** by cryptand **12** is nearly 6-times higher than any other reported host.

Introduction

Crown ether-based molecular recognition¹ has been a goal since Pedersen's first report of crown ether binding of alkali metal ions.² In the mid-1980s, Stoddart and co-workers reported that *cis*(4,4′)-disubstituted dibenzo-30-crown-10 crown ethers (**1**) are good hosts for dimethyl paraquat and diquat (**3b** and **4**,

respectively), but the synthesis of diol **1d** via **1b** was low yielding.³ From **1d**, Stoddart et al. synthesized a cryptand, **6**, which significantly improved binding of **4** due to the addition of binding sites and preorganization of the host.⁴ Likely due to synthetic challenges of making cryptands and functional diquats, little work has been done with these systems since the 1980s.

The Gibson group has spent the past 10 years working on creating synthetically accessible crown ethers⁵ and cryptands⁶ that have specific and strong interactions with guests **3** and **4** and monopyridinium guests. Our overall goal is then to use these binding interactions to build supramolecular polymers.⁷ We previously reported a pyridyl cryptand, **8**, made via bis(*meta*-

(1) Reviews: (a) Vögtle, F. *Supramolecular Chemistry*; John Wiley and Sons: New York, 1991. (b) Cram, D. J.; Cram, J. M. *Container Molecules and Their Guests*; Royal Society of Chemistry: Cambridge, UK, 1994. (c) Lehn, J.-M. *Supramolecular Chemistry*; VCH Publishers: New York, 1995. (d) *Comprehensive Supramolecular Chemistry*; Atwood, J. L., Davies, J. E. D., MacNicol, D. D., Vögtle, F., Exec. Eds.; Pergamon Press: New York, 1996. (e) *Monographs in Supramolecular Chemistry: Self-Assembly in Supramolecular Systems*; Lindoy, L. F., Atkinson, I. M., Eds.; Royal Society of Chemistry: London, UK, 2000. (f) *Supramolecular Chemistry*; Steed, J. W., Atwood, J. L., Eds.; J. Wiley and Sons: New York, 2000. (g) Rudkevich, D. M. *Angew. Chem., Int. Ed.* **2004**, *43*, 558–571. Individual papers of note: (h) Lehn, J.-M. *Science* **2002**, *295*, 2400–2403. (i) Reinhoudt, D. N.; Crego-Calama, M. *Science* **2002**, *295*, 2403–2407. (j) Zimmerman, S. C.; Wendland, M. S.; Rakow, N. A.; Zharov, I.; Suslick, K. S. *Nature* **2002**, *418*, 399–403. (k) Hernandez, J. V.; Kay, E. R.; Leigh, D. A. *Science* **2004**, *306*, 1532–1537. (l) Kay, E. R.; Leigh, D. A. *Nature* **2006**, *440*, 286–287.

(2) (a) Pedersen, C. J. *J. Am. Chem. Soc.* **1967**, *89*, 2495–2496. (b) Pedersen, C. J. *J. Am. Chem. Soc.* **1967**, *89*, 7017–7036. (c) Pedersen, C. J. *J. Am. Chem. Soc.* **1970**, *92*, 391–394. (d) Pedersen, C. J. *Org. Synth.* **1972**, *52*, 66–74.

(3) (a) Colquhoun, H. M.; Goodings, E. P.; Maud, J. M.; Stoddart, J. F.; Williams, D. J.; Wolstenholme, J. B. *J. Chem. Soc., Chem. Commun.* **1983**, 1140–1142. (b) Kohnke, F. H.; Stoddart, J. F.; Allwood, B. L.; Williams, D. J. *Tetrahedron Lett.* **1985**, *26*, 1681–1684. (c) Kohnke, F. H.; Stoddart, J. F. *Tetrahedron Lett.* **1985**, *26*, 1685–1658. (d) Colquhoun, H. M.; Goodings, E. P.; Maud, J. M.; Stoddart, J. F.; Wolstenholme, J. B.; Williams, D. J. *J. Chem. Soc., Perkin Trans.* **1985**, *2*, 607–624.

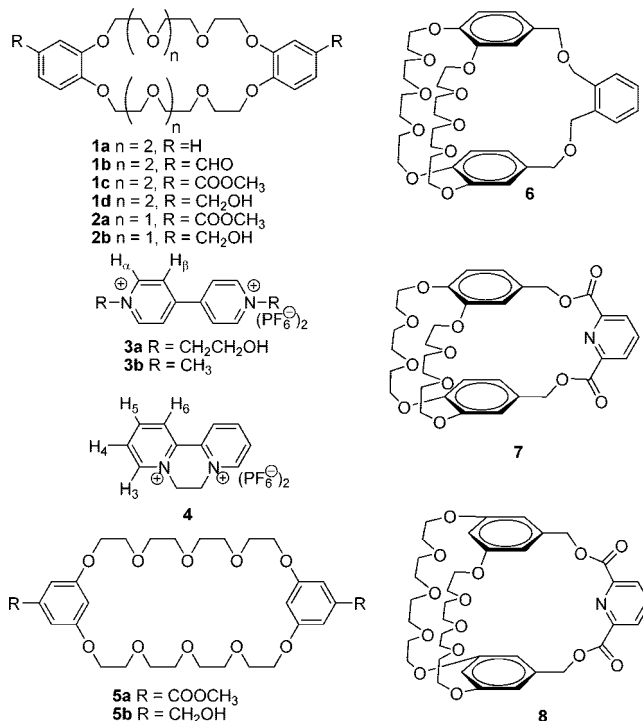
(4) (a) Allwood, B. L.; Kohnke, F. H.; Slawin, A. M. Z.; Stoddart, J. F.; Williams, D. J. *J. Chem. Soc., Chem. Commun.* **1985**, 311–314. (b) Kohnke, F. H.; Stoddart, J. F. *J. Chem. Soc., Chem. Commun.* **1985**, 314–317. (c) Allwood, B. L.; Kohnke, F. H.; Stoddart, J. F.; Williams, D. J. *Angew. Chem.* **1985**, *97*, 584–587.

phenylene)-32-crown-10 derivatives **5a** and **5b**, that complexed paraquat **3b** with an association constant, $K_a = 5 \times 10^6 \text{ M}^{-1}$ (in acetone, 22 °C).^{6b} However, the synthesis of precursor **5a** is tedious and low-yielding.^{5a} We began to seek alternative hosts that were more readily synthesized and complexed guests **3** and/or **4** equally strongly. We previously reported a high-yielding regioselective synthesis of *cis*-(4,4')-di(carbomethoxybenzo)-24-crown-8 (**2a**);^{5c} however, disappointingly the cryptand **7** made from **2a** was less able to bind paraquat ($1.0 \times 10^4 \text{ M}^{-1}$ in acetone at 22 °C) than the larger host **8** and does not appear to bind diquat at all due to steric effects.^{6d}

Having an excellent methodology for regioselective syntheses of symmetrical “*cis*-(4,4')”-disubstituted dibenzocrown ethers^{5e} and the knowledge that the 32-membered bis(*m*-phenylene)-based cryptand afforded very high association constants with paraquats, we naturally were drawn to consider the analogous 30-membered dibenzocrown ether-based cryptand **12** as potentially possessing the best of both worlds: facile synthetic accessibility and powerful binding of paraquats and diquats. CPK models indicated that cryptand **12** would be a good host for paraquats. In this paper we show that the same synthetic method used to synthesize dibenzo-24-crown-8 derivative **2a** does, in fact, work extremely well for the larger dibenzo-30-crown-10 diester **1c** and we show that cryptand **12**, derived from **1c**, is a better host for both guests **3** and **4** than dibenzo-24-crown-8-derived cryptand **7**^{6d} and nearly as good as bis(*m*-phenylene)-32-crown-10-derived cryptand **8** for paraquats (**3**). Interestingly cryptand **12** complexes diquat (**4**) more powerfully than any previously reported host.

To produce supramolecular polymers one must have a synthetically available system with good solubility and very high association constants.^{7e,8} In this paper we report a synthetically accessible host which does not have the significant solubility issues of the cyclodextrin and cucurbituril systems,⁹ and binds paraquat and diquat well enough to afford true supramolecular

polymers. To date, diquats have not been employed as widely as paraquats in such self-assembly process, but recently Pd catalyzed coupling to form functional 2,2'-bipyridines has been vastly improved,¹⁰ allowing for synthesis of functional diquats for use in the production of supramolecular polymers.



Results and Discussion

Synthesis of Cryptand 12. We previously reported the synthesis of methyl 3-hydroxy-4-benzyloxybenzoate (**9**) from the methyl 3,4-dihydroxy benzoate.^{5e} The coupling of **9** with tetra(ethylene glycol) ditosylate to make dimer **10** proceeds quickly and in high yield (Scheme 1). The hydrogenolysis of dibenzyl ether **10** affording the key bisphenol **11** is complete within a couple of hours with quantitative yield. The cyclization of bisphenol **11** with tetra(ethylene glycol) ditosylate is templated well in refluxing acetonitrile by the highly soluble KPF₆ and poorly soluble K₂CO₃, affording the desired crown ether diester **1c** in 93% yield by mixing the components from the start, i.e., without resorting to pseudo-high dilution. The yield in this cyclization is higher than that reported (89%) for the 24-membered analog **2a**;^{5c} however, in the latter case the potassium salt was isolated in quantitative yield. Given the relative association constants for potassium ion with dibenzo-24-crown-8 (average $7.6 \times 10^3 \text{ M}^{-1}$)¹¹ and dibenzo-30-crown-10 (average $4.3 \times 10^4 \text{ M}^{-1}$)¹² in acetonitrile and the fact that the reactions

(5) (a) Gibson, H. W.; Nagvekar, D. S. *Can. J. Chem.* **1997**, *75*, 1375–1384. (b) Bryant, W. S.; Guzei, I. A.; Rheingold, A. L.; Gibson, H. W. *Org. Lett.* **1999**, *1*, 47–50. (c) Jones, J. W.; Zakharov, L. N.; Rheingold, A. L.; Gibson, H. W. *J. Am. Chem. Soc.* **2002**, *124*, 13378–13379. (d) Huang, F.; Zakharov, L. N.; Rheingold, A. L.; Jones, J. W.; Gibson, H. W. *Chem. Commun.* **2003**, 2122–2123. (e) Gibson, H. W.; Wang, H.; Bonrad, K.; Jones, J. W.; Slebońnick, C.; Zakharov, L. N.; Rheingold, A. L.; Habenicht, B.; Lobue, P.; Ratliff, A. E. *Org. Biomol. Chem.* **2005**, *3*, 2114–2121. (f) Huang, F.; Guzei, I. A.; Jones, J. W.; Gibson, H. W. *Chem. Commun.* **2005**, 1693–1695. (g) Huang, F.; Zakharov, L. N.; Rheingold, A. L.; Ashraf-Khorassani, M.; Gibson, H. W. *J. Org. Chem.* **2005**, *70*, 809–813, and references therein.

(6) (a) Bryant, W. S.; Jones, J. W.; Mason, P. E.; Guzei, I.; Rheingold, A. L.; Fronczek, F. R.; Nagvekar, D. S.; Gibson, H. W. *Org. Lett.* **1999**, *1*, 1001–1004. (b) Huang, F.; Switek, K. A.; Zakharov, L. N.; Fronczek, F. R.; Slebońnick, C.; Lam, M.; Golen, J. A.; Bryant, W. S.; Mason, P. E.; Rheingold, A. L.; Ashraf-Khorassani, M.; Gibson, H. W. *J. Org. Chem.* **2005**, *70*, 3231–3241. (c) Huang, F.; Slebońnick, C.; Switek, K. A.; Gibson, H. W. *Chem. Commun.* **2006**, 1929–1931. (d) Gibson, H. W.; Wang, H.; Slebońnick, C.; Merola, J.; Kassel, W. S.; Rheingold, A. L. *J. Org. Chem.* **2007**, *72*, 3381–3393. (e) Huang, F.; Slebońnick, C.; Switek, K. A.; Gibson, H. W. *Tetrahedron* **2007**, *63*, 2829–2839. (f) Huang, F.; Slebońnick, C.; Mahan, E. J.; Gibson, H. W. *Tetrahedron* **2007**, *63*, 2875–2881. (g) Pederson, A. M.-P.; Vektor, R. C.; Rouser, M. A.; Huang, F.; Slebońnick, C.; Schoonover, D. V.; Gibson, H. W. *J. Org. Chem.* **2008**, *73*, 5570–5573, and references therein.

(7) (a) Huang, F.; Gibson, H. W. *Prog. Polym. Sci.* **2005**, *30*, 982–1018. (b) Huang, F.; Gibson, H. W. *Chem. Commun.* **2005**, 1696–1698. (c) Gibson, H. W.; Ge, Z.; Huang, F.; Jones, J. W.; Lefebvre, H.; Vergne, M. J.; Hercules, D. M. *Macromolecules* **2005**, *38*, 2626–2637. (d) Huang, F.; Nagvekar, D. S.; Slebońnick, C.; Gibson, H. W. *J. Am. Chem. Soc.* **2005**, *127*, 484–485. (e) Huang, F.; Nagvekar, D. S.; Zhou, X.; Gibson, H. W. *Macromolecules* **2007**, *40*, 3561–3567, and references therein.

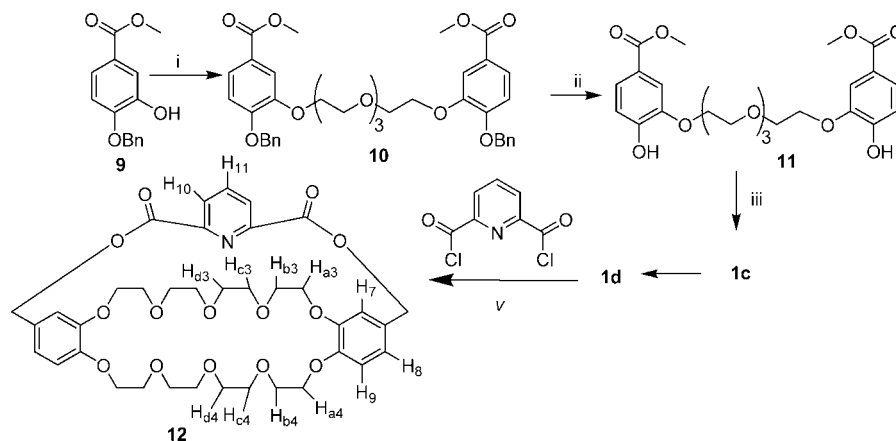
(8) Sijbesma, R. P.; Beijer, F. H.; Brunsveld, L.; Folmer, B. J. B.; Hirschberg, J. H. K. K.; Lange, R. F. M.; Lowe, J. K. L.; Meijer, E. W. *Science* **1997**, *278*, 1601–1604.

(9) (a) Nepogodiev, S. A.; Stoddart, J. F. *Chem. Rev.* **1998**, *98*, 1959–1976. (b) Kim, K.; Selvapalam, N.; Ko, Y. H.; Park, K. M.; Kim, D.; Kim, J. *Chem. Soc. Rev.* **2007**, *36*, 267–279.

(10) (a) Savage, S. A.; Smith, A. P.; Fraser, C. L. *J. Org. Chem.* **1998**, *63*, 10048–10051. (b) Lützen, A.; Hapke, M. *Eur. J. Org. Chem.* **2002**, 2292–2297. (c) Lützen, A.; Hapke, M.; Staats, H.; Bunzen, J. *Eur. J. Org. Chem.* **2003**, 394, 8–3957. (d) Newkome, G. R.; Patri, A. K.; Holder, E.; Schubert, U. S. *Eur. J. Org. Chem.* **2004**, 235–254.

(11) (a) Takeda, Y. *Bull. Chem. Soc. Jpn.* **1983**, *56*, 3600–3602. (b) Takeda, Y.; Kudo, Y.; Fujiwara, S. *Bull. Chem. Soc. Jpn.* **1985**, *58*, 1315–1316. (c) Tawarrah, K. M.; Mizyed, S. A. *J. Solution Chem.* **1989**, *18*, 387–401. (d) Chantooni, M. K., Jr.; Roland, G.; Kolthoff, I. M. *J. Solution Chem.* **1988**, *17*, 175–189. (e) Izatt, R. M.; Pawlak, K.; Bradshaw, J. S.; Bruening, R. L. *Chem. Rev.* **1991**, *91*, 1720–2085.

(12) (a) Massaux, J.; Roland, G.; Desereux, J. F. *J. Solution Chem.* **1982**, *11*, 549–555. (b) Chantooni, M. K., Jr.; Roland, G.; Kolthoff, I. M. *J. Solution Chem.* **1988**, *17*, 175–189.

SCHEME 1. Synthesis of **12**^a

^a (i) Ts(OCH₂CH₂)₄OTs, 2 equiv K₂CO₃, CH₃CN, reflux/12 h, 93%; (ii) H₂, Pd/C, 99%; (iii) Ts(OCH₂CH₂)₄OTs, 1 equiv KPF₆, 5 equiv K₂CO₃, CH₃CN, reflux/12 h, 93%; (iv) LiAlH₄, THF, 94%; (v) CH₂Cl₂/pyridine, pseudo-high dilution, 25°C, 6 days, 44%.

were carried out at 44 and 57 mM, respectively, it is not surprising that the yield of **1c** may be higher. The overall yield of **1c** from **9** is 86% and the synthesis was accomplished in less than 3 days; Huang et al. reported the preparation of **1c** via tetra(ethylene glycol) dichloride with K₂CO₃ only (no KPF₆) over a period of 9.5 days in 44% overall yield.¹³ The structure of **1c** was confirmed by ¹H NMR and positive ion high resolution fast atom bombardment mass spectrometry (FAB-MS).

The crown ether diester **1c** was converted in high yield to the diol **1d** via reaction with lithium aluminum hydride in dry THF. Diol **1d** was reacted with pyridine 2,6-dicarboxylic acid chloride under pseudo-high dilution conditions, leading to pure cryptand **12** in 44% yield. FAB-MS and ¹H NMR of crude **12** demonstrated the presence of a complex with the pyridinium ion; based on this observation, we are working on templation to increase the yield of this final step.

The ¹H NMR spectrum of cryptand **12** shows that it has the same C₂ symmetry as 24-crown analog **7**,^{6d} the signal for the benzylic methylene hydrogens is a singlet and the two non-equivalent ethyleneoxy arms are well-resolved (Figure 1). **12** was also analyzed by FAB-MS: *m/z* 727.2874 (error 4.7 ppm) for [**12**]⁺.

Single crystals of cryptand **12** were grown by slow evaporation of a 9:1 (v:v) chloroform:acetone solution at rt. The crystal

structure of **12**¹⁴ shows that it is slightly collapsed, but its cavity is accessible (Figure 2); the structure shows an absence of solvent molecules around or in the cryptand. The catechol rings are offset by about 3.1 Å, nonparallel by 18.72°, and the centroid-centroid distance is 5.458 Å.

Complexation of Paraquat Diol (3a) by Cryptand 12. The complex **12·3a** is yellow due to charge transfer interactions between the electron rich benzo rings of the host and the electron deficient pyridinium rings of the guest; the host and guest are colorless individually. The strength of complexation was measured by isothermal titration calorimetry (ITC); Δ*H* = −13(±1) kcal/mol and an association constant (*K*_a) of 1.0(±0.1) × 10⁵ M^{−1} were determined in acetone at 22 °C. The 1:1 stoichiometry of the complex was also confirmed by FAB-MS: *m/z* 1118.3832 [**12·3a** − PF₆]⁺ (error 1.6 ppm); no other stoichiometries were detected. 1D NOE experiments show the through-space interactions of H_α and H_β of the guest (**2a**) with the aromatic and ethyleneoxy protons of the host (**12**) in the solution phase.

The complexation of **3a** with **12** was also investigated via ¹H NMR spectroscopy (Figure 3). The aromatic signals of

(13) He, C.; Shi, Z.; Zhou, Q.; Li, S.; Li, N.; Huang, F. *J. Org. Chem.* **2008**, *73*, 5872–5880.

(14) Colorless plates (0.24 × 0.19 × 0.05 mm³) of **12** crystallized from 9:1 chloroform/acetone by slow evaporation at room temperature. The chosen crystal was centered on the goniometer of an Oxford Diffraction Gemini S Ultra diffractometer operating with Cu Kα radiation. The data collection routine, unit cell refinement, and data processing were carried out with the program CrysAlisPro.¹⁵ The Laue symmetry was consistent with the triclinic space groups *P1* and *P1̄*. The structure was solved by direct methods and preliminary refinements performed in both *P1* and *P1̄* using SHELXTL NT.¹⁸ The original refinement models in both *P1* and *P1̄* suggested the same disorder in the crystal structure. Therefore, the higher symmetry space group, *P1̄*, was chosen. The asymmetric unit of the structure comprises two host–guest complexes, two water molecules and one acetone molecule. The final refinement model involved anisotropic displacement parameters for all ordered non-hydrogen atoms and a riding model for all hydrogen atoms.

(15) CrysAlisPro, v1.171.32; Oxford Diffraction: Wroclaw, Poland, 2007.

(16) Altomare, A.; Burla, M. C.; Camalli, G.; Cascarano, G.; Giacovazzo, C.; Guagliardi, A.; Moliterni, A. G. G.; Polidori, G.; Rizzi, R. *J. Appl. Crystallogr.* **1999**, *32*, 115–119.

(17) Farrugia, L. J. *J. Appl. Crystallogr.* **1999**, *32*, 837–838.

(18) Sheldrick, G. M. *Acta Crystallogr.* **2008**, *A64*, 112–122.

(19) Tsukube, H.; Furuta, H.; Odani, A.; Takeda, Y.; Kudo, Y.; Inoue, Y.; Liu, Y.; Sakamoto, H.; Kimura, K. In *Comprehensive Supramolecular Chemistry*; Atwood, J. L., Davies, J. E. D., MacNicol, D. D., Vögtle, F., Eds.; Pergamon Press: London, 1996; Vol. 8, pp 425–482.

(20) Yellow blocks (0.07 × 0.24 × 0.27 mm³) of **12·3a** crystallized from acetone/pentane by vapor diffusion at room temperature. The chosen crystal was centered on the goniometer of an Oxford Diffraction Xcalibur S diffractometer operating with Mo Kα radiation. The data collection routine, unit cell refinement, and data processing were carried out with the program CrysAlis.¹⁵ The Laue symmetry was consistent with the triclinic space groups *P1* and *P1̄*. The structure was solved by direct methods and preliminary refinements performed in both *P1* and *P1̄* using SHELXTL NT.¹⁸ The original refinement models in both *P1* and *P1̄* suggested the same disorder in the crystal structure. Therefore, the higher symmetry space group, *P1̄*, was chosen. The asymmetric unit of the structure comprises two host–guest complexes, two water molecules and one acetone molecule. The final refinement model involved anisotropic displacement parameters for all ordered non-hydrogen atoms and a riding model for all hydrogen atoms. The hydrogen atoms from the water molecules could not be located in the residual electron density map and were not included in the refinement. Two-position disorder models were used for the arm of one host molecule, one guest molecule, and two PF₆[−]. The disordered atoms in the arm of a host molecule were refined isotropically to relative occupancies of 0.640(7) and 0.360(7). Both disordered PF₆[−] were refined anisotropically. The relative occupancies of the P4 containing PF₆[−] refined to 0.46(2) and 0.54(2). The P3 containing PF₆[−] is disordered near an inversion center such that PF₆[−] cannot be in both positions at once, so the occupancies were constrained to 0.50. The disorder in the guest molecule is coupled to the disorder in this PF₆[−] and the occupancies of the guest were also constrained to 0.50. This guest molecule was refined isotropically. After modeling the disorder, a region with weak residual electron density peaks (1–2 e[−]/Å³) could not be modeled as anything chemically reasonable and the peaks were assumed to arise from partially evaporated solvent. The SQUEEZE subroutine of the PLATON program package was used and a total of 8 e[−] was subtracted from 284.8 Å³ of void space.²¹

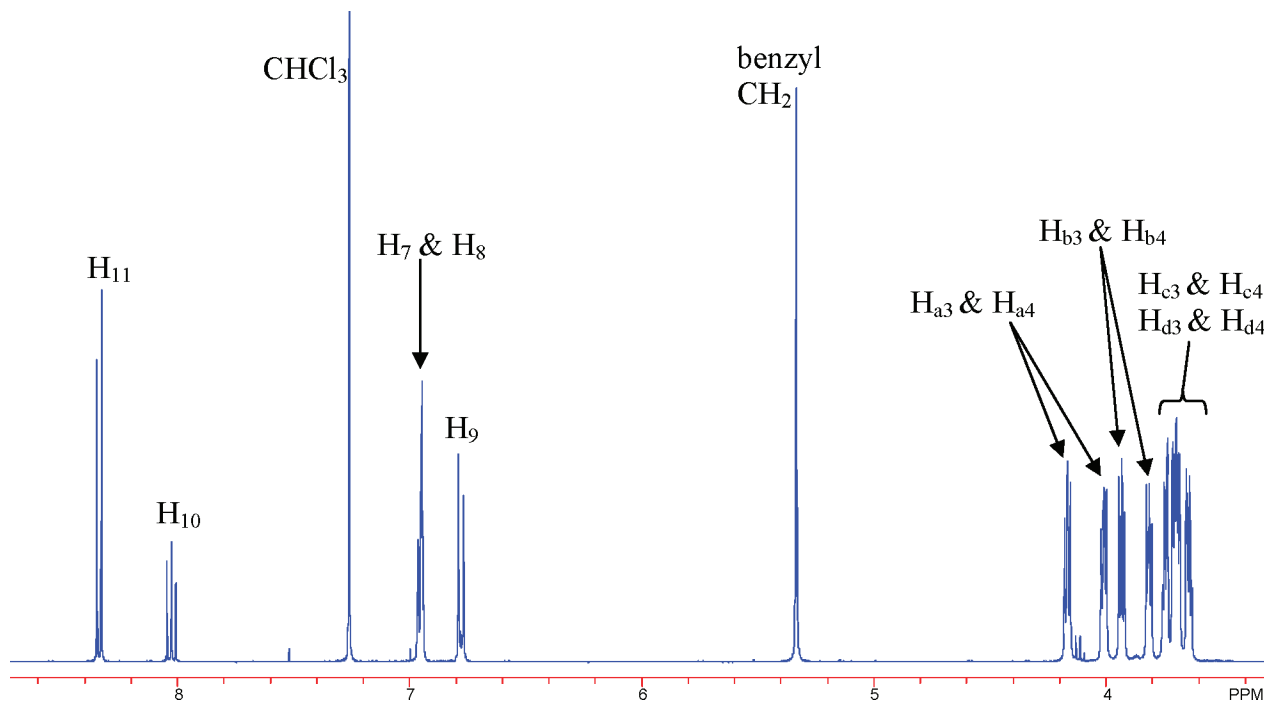


FIGURE 1. ^1H NMR spectrum (400 MHz) of cryptand **12** in CDCl_3 .

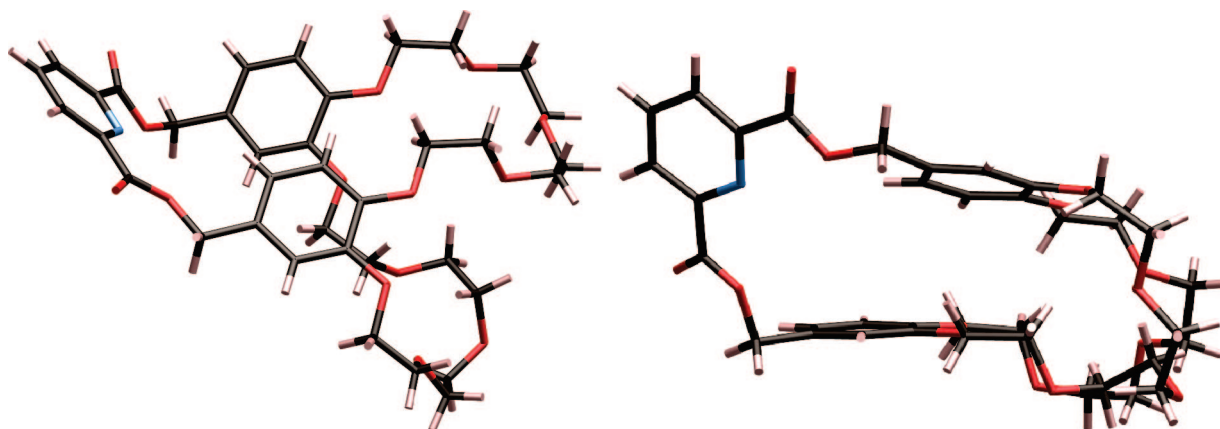


FIGURE 2. Top and side views of the X-ray crystal structure of **12**.

cryptand **12** are shifted upfield upon complexation, as usually observed in such complexes.^{4–6} The similarity of the results for 1:1 compared to 1:70 host:guest stoichiometry shows that binding is strong. With such strong binding ($K_a > 10^4 \text{ M}^{-1}$), the association constant cannot be accurately determined by ^1H NMR directly.¹⁹ The complexation of guest **3a** by host **12** was also investigated by ^1H NMR in $\text{DMSO}-d_6$: $K_a = 125 (\pm 25) \text{ M}^{-1}$ which is impressive in this competitive hydrogen bonding, polar solvent.

Crystals of **12**·**3a** were grown by vapor diffusion of pentane into an acetone solution of the complex at rt. The crystal structure (Figure 4) reveals two distinct dimorphs.²⁰ In dimorph I the pyridyl-N is interacting with two H_β s (shown by lines **a** and **b**) of **3a**, which is threaded through the cavity nearly orthogonal to the pyridyl ring; the 3-position arm of **12** is interacting with one H_α (shown by line **c**) and one N^+CH_2 (shown by line **d**) of **3a**, and the 4-position ethyleneoxy arm of **12** is not interacting with **3a**, but is interacting with a water

molecule which is then strongly interacting with two H_β s of **3a** [similar to the **12**·**3b** dimorphs described below (Figure 5)]; we have reported similar findings previously.^{6a} In dimorph II one end of the guest resides in the cavity of the crown ether macrocycle of **12** and the guest lies at an oblique angle with respect to the pyridyl ring; the pyridyl-N is interacting with an H_α (shown by line **e**) and an H_β (shown by line **f**) of **3a**; the third oxygen of the 3-position arm of host **12** is interacting with an H_α (shown by line **h**) and N^+CH_2 (shown by line **i**), and the 4-position arm is interacting with an H_α (shown by line **g**).

Complexation of Dimethyl Paraquat (**3b**) with Cryptand **12**.

The complex **12**·**3b** is yellow due to charge transfer interactions between the electron rich benzo rings of the host and the electron poor pyridinium rings of the guest. The strength of complexation was measured by ITC; $\Delta H = -14(\pm 1) \text{ kcal/mol}$ and an association constant (K_a) of $2.0(\pm 0.2) \times 10^5 \text{ M}^{-1}$ were determined in acetone at 22 °C. The 1:1 stoichiometry of the complex was confirmed by FAB-MS: m/z 1058.3671[**12**·**3b** – PF_6]⁺ (error 3.0 ppm); no other stoichiometries were detected. 1D NOE experiments show the through-space interactions of

(21) Spek, A. L. *J. Appl. Crystallogr.* **2003**, *36*, 7–13.

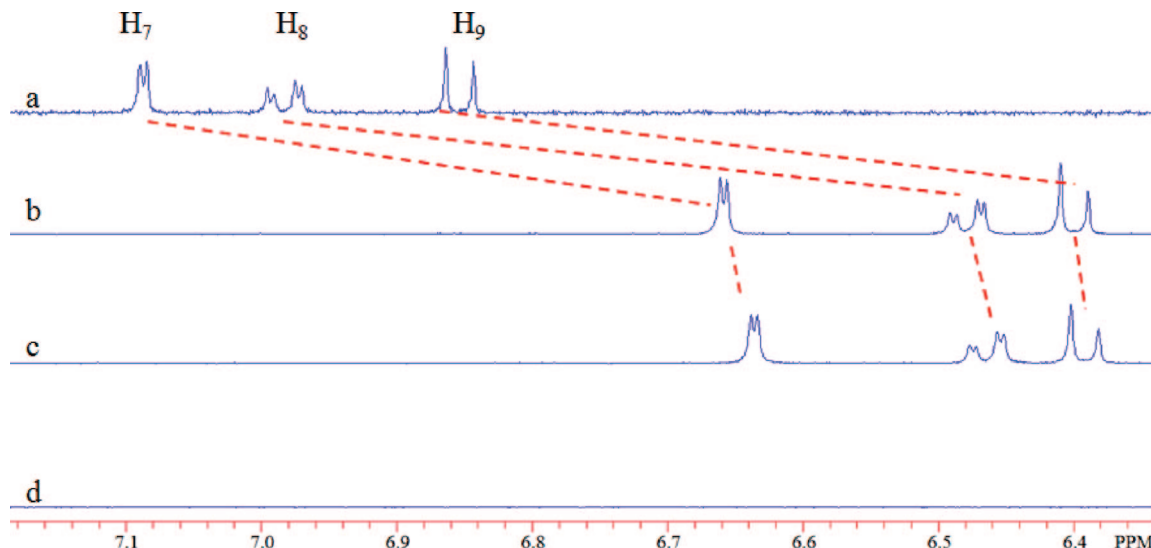


FIGURE 3. Partial ^1H NMR spectra of cryptand **12** and paraquat diol (**3a**) in acetone- d_6 at 23 $^\circ\text{C}$. (a) 1.00 mM **12**, (b) 1.00 mM **12** and **3a**, (c) 1.00 mM **12** and 70.0 mM **3a**, (d) 1.00 mM **3a**.

H_α and H_β of the guest with the aromatic and ethyleneoxy protons of host **12** in the solution phase.

Crystals of **12**·**3b** were grown by vapor diffusion of pentane into an acetone solution of the complex at rt. The crystal structure (Figure 5) shows that the complex exists as two dimorphs in the solid state.²² However, unlike the situation with **12**·**3a** the dimorphs have only subtle differences in the cryptand's ethyleneoxy arms. The pyridyl-N interacts with two H_β of dimethyl paraquat (shown by lines **a**, **b**, **e** and **f**) and the 3-position arm of **12** interacts with one H_α (shown by lines **c** and **g**) and one of the methyl protons (shown by lines **d** and **h**) of **3b** in both dimorphs. The solid phase structure shows that the 4-position ethyleneoxy arm of cryptand **12** does not interact with guest **3b** in either dimorph which is the same as in the complex **12**·**3a** (Figure 4). We believe this is the reason the association constant values of dibenzo-30-crown-8-derived cryptand **12** with these paraquat species are less than the one from our previously reported highly associating, analogous bis(*m*-phenylene)-32-crown-10-based cryptand **8** ($K_a = 5 \times 10^6 \text{ M}^{-1}$);^{6b} the *ortho*-linkage in **12** does not allow both ethyleneoxy

arms to interact with the guest, while the *meta*-orientation of the ethyleneoxy units in the latter does allow such interaction.

Complexation of Diquat (4) with Cryptand 12. This system was examined on the basis that the broader diquat molecule might engage both ethyleneoxy arms of cryptand **12**, affording a "tighter binding" than with the narrower paraquats (**3**). The complex **12**·**4** is orange-red due to charge transfer interactions between the electron rich benzo rings of the host and the electron deficient pyridinium rings of the guest. The strength of complexation was measured by ITC; $\Delta H = -14(\pm 1) \text{ kcal/mol}$ and $K_a = 1.9(\pm 0.6) \times 10^6 \text{ M}^{-1}$ were determined in acetone at 25 $^\circ\text{C}$. This is the highest association constant ever reported for guest **4**; previously we reported that the bis(*m*-phenylene)-32-crown-10-based cryptand **8** binds diquat (**4**) with $K_a = 3.3 \times 10^5 \text{ M}^{-1}$ (acetone, 22 $^\circ\text{C}$) measured by a competitive NMR method.^{6c} With regard to our overall aim of constructing supramolecular polymers this is a significant improvement; for example, in a system comprised of complementary homoditopic monomers at 10 mM concentration, the dihost with individual $K_a = 3.3 \times 10^5 \text{ M}^{-1}$ would produce oligomeric material containing on average only 57 repeat units (n), while the new cryptand-based dihost would lead to a true polymeric species with $n = 1.4 \times 10^2$ repeat units (calculated from $n = \{K_a[\text{conc}]\}^{1/2}$).^{7e,8} Moreover, the development of a facile

(22) Yellow plates ($0.03 \times 0.17 \times 0.23 \text{ mm}^3$) of **12**·**3b** crystallized from acetone/ethyl acetate at room temperature. The chosen crystal was centered on the goniometer of an Oxford Diffraction Gemini S diffractometer operating with Cu K α radiation. The data collection routine, unit cell refinement, and data processing were carried out with the program CrysAlis.¹⁵ The Laue symmetry was consistent with the triclinic space groups $P\bar{1}$ and $P1$. The centric space group $P\bar{1}$ was chosen based on the $|E^2 - 1|$ value ($|E^2 - 1| = 1.027$). The structure was solved by direct methods and refined using SHELXTL NT.¹⁸ The asymmetric unit of the structure comprises 2 host-guest complexes, 3 water molecules, and 2.7 acetone molecules. The final refinement model involved anisotropic displacement parameters for non-hydrogen atoms and a riding model for all hydrogen atoms. The hydrogen atoms from the water molecules could not be located in the residual electron density map and were not included in the refinement. The original refinement model suggested substantial disorder in the crystal structure. A 2-position disorder model was used for one arm of a host molecule and the $P3$ containing PF_6 anion; because this disorder was located near an inversion center, both positions cannot be occupied simultaneously and the relative occupancies were constrained to 50%. Atom C(13) of a host molecule was modeled as 2-position disorder with relative occupancies 0.627(15) and 0.373(15). The P(4) containing PF_6 anion was also modeled as 2-position disorder with relative occupancies 0.572(10) and 0.428(10). The displacement ellipsoid drawing suggested additional disorder in the P(5) containing PF_6 anion and two acetone molecules. Attempts to model this disorder did not improve the refinement and were abandoned. Because of extremely large thermal parameters, the occupancy of the acetone molecule containing O(34) was allowed to refine and converged to 0.695(12).

(23) Orange plates ($0.07 \times 0.15 \times 0.20 \text{ mm}^3$) of **12**·**4** crystallized from acetone/pentane by vapor diffusion at room temperature. The chosen crystal was centered on the goniometer of an Oxford Diffraction Gemini S diffractometer operating with Mo K α radiation. The data collection routine, unit cell refinement, and data processing were carried out with the program CrysAlis.¹⁵ The Laue group was consistent with the triclinic space groups $P\bar{1}$ and $P1$. The structure was solved direct methods in both $P\bar{1}$ and $P1$ and refined using SHELXTL NT.¹⁸ Preliminary refinements suggested disorder with both space groups; the centric space group $P1$ was chosen. In $P1$, the asymmetric unit of the structure comprises one crystallographically independent $[\text{C}_{37}\text{H}_{45}\text{NO}_{14} \cdot \text{C}_{12}\text{H}_{12}\text{N}_2][\text{PF}_6]_2$. The final refinement model involved anisotropic displacement parameters for all non-hydrogen atoms except the fluorine atoms of the PF_6 anions. A riding model was used for all hydrogen atoms. Residual electron density maps suggested substantial disorder of the PF_6 anions and disorder in the host molecule. One PF_6 anion was modeled with 3-position disorder with relative occupancies that refined to 0.516(4), 0.296(8), and 0.188(8). The second PF_6 anion was modeled with 2-position disorder with occupancies that refined to 0.500(5). Both anions were restrained to be octahedral using the SADI command in SHELXL-97. Although the displacement ellipsoids of the host molecule suggest additional disorder, discrete disorder sites in the host could not be found and attempts to model this disorder were abandoned.

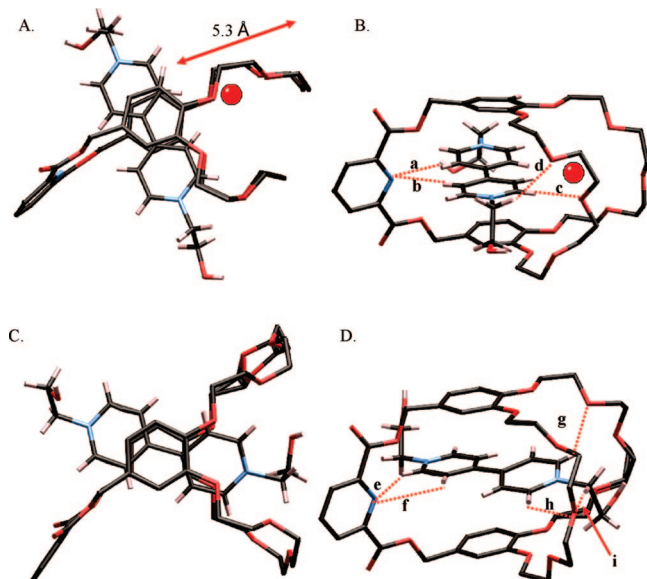


FIGURE 4. Top (A and C) and side (B and D) views of the X-ray crystal structure of the dimorphs of **12·3a**. The PF_6^- counterions, solvent molecules, and hydrogens of **12** were omitted. Dimorph I (A and B) is not disordered. Both guest **3a** and the 4-position ethyleneoxy arm of **12** are disordered (disorder in **3a** not shown) in dimorph II (C and D). All PF_6^- counterions are disordered. $\text{C}\cdots\text{O}(\text{N})$ distances (Å) and angles ($^\circ$) for H-bonds: **a** 3.568, 176.7; **b** 3.483, 170.3; **c** 3.085, 167.3; **d** 3.380, 150.4; **e** 3.231, 139.3; **f** 3.528, 109.5; **g** 3.173, 133.2; **h** 3.782, 134.9; **i** 3.104, 169.3. The disordered guest, **3a**, has similar interactions (**e**, **g**, **h**, **i**) with **12** of dimorph II. In dimorph I, both of the ester sp^3 -oxygens of host **12** have weak interactions with H_β of **3a**; the $\text{C}\cdots\text{O}$ distances vary from 3.172–3.577 Å and the angles vary from 116–128°. The catechol rings of dimorphs I and II are stacked and the centroid-centroid distances (Å) are 6.903 and 6.813, respectively. The distances (Å) between the catechol centroids and the plane of the guest molecule are 3.365 and 3.437 for dimorph I and 3.358 and 3.449 for dimorph II. The angles ($^\circ$) between each catechol and the plane of the guest molecule are 4.35 and 7.67 for dimorph I and 3.69 and 3.71 for dimorph II. The red double-headed arrow in A shows the 4-position ethyleneoxy arm of **12** of dimorph I that is too far away to interact with **3a** directly; this arm is holding a water molecule, the red sphere shows the oxygen atom of water [$\text{O}\cdots\text{O}$ distances (Å) 2.865 and 2.867; $\text{O}\cdots\text{O}\cdots\text{O}$ angle 108.9°] which is closely interacting with two H_β s of **3a** [$\text{C}\cdots\text{O}$ distances (Å) and $\text{C}-\text{H}\cdots\text{O}$ angles ($^\circ$) are: 3.235, 176.6 and 3.263, 175.6].

synthesis of precursor **1c** for **12** also represents a significant advance versus the tedious preparation of precursor **5a** for **8**. The 1:1 stoichiometry of the **12·4** complex was confirmed by FAB-MS: m/z 1056.3531 [**12·4** - PF_6] $^+$ (error 4.6 ppm); no other stoichiometry was detected. 1D NOE experiments show the through-space interactions of the guest's ethylene protons with the ethyleneoxy protons of host **12** in the solution phase.

Crystals of **12·4** were grown by vapor diffusion of pentane into an acetone solution of the complex at rt. The crystal structure²³ shows all four ethylene protons of guest **4** have bifurcated H-bond interactions (shown by lines **c/d**, **e/f**, **g/h**, **i/j**), engaging both of the ethyleneoxy arms of cryptand **12**, as anticipated. H_6 of guest **4** is also interacting with an ethyleneoxy arm of host **12** (shown by line **k**). The pyridyl nitrogen of host **12** interacts with H_5 (shown by line **b**) and H_6 (shown by line **a**) of guest **4**. The other 6-, 5-, and both of the 4-position protons of guest **4** are not bound to host **12** in the solid state.

Complexation of 3b with 12. The complex of dimethyl paraquat (**3b**) and bis(*m*-phenylene)-32-crown-10-derived cryptand **8** was previously described via its X-ray crystal structure and

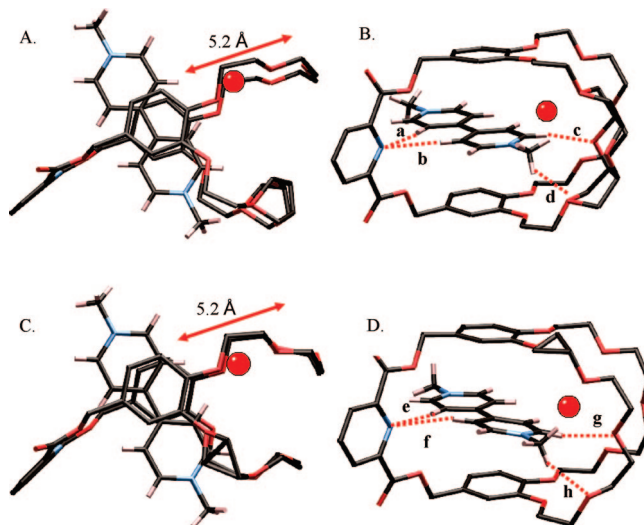


FIGURE 5. Top (A and C) and side (B and D) views of the X-ray crystal structure of the dimorphs of **12·3b**. The PF_6^- counterions, solvent molecules, and hydrogens of **12** were omitted. Five atoms of the 3-position ethyleneoxy arm of **12** of dimorph I (A and B) are disordered; only one atom of the 3-position ethyleneoxy arm of **12** of dimorph II (C and D) is disordered. All PF_6^- counterions are disordered. $\text{C}\cdots\text{O}(\text{N})$ distances (Å) and angle ($^\circ$) for H-bonds: **a** 3.627, 173.0; **b** 3.561, 170.2; **c** 3.082, 165.6; **d** 3.581, 154.6; **e** 3.338, 168.0; **f** 3.609, 165.6; **g** 3.169, 166.2; **h** 3.319, 141.2. In both dimorphs, both of the ester sp^3 -oxygens of host **12** have weak interactions with H_β of guest **3b**; the $\text{C}\cdots\text{O}$ distances vary from 3.078–3.612 Å and angles vary from 111–134°. The catechol rings of I and II are stacked and the centroid-centroid distances (Å) are 6.932 and 6.829, respectively. The distances (Å) between the catechol centroids and the plane of the guest molecule are 3.384 and 3.515 for dimorph I and 3.380 and 3.520 for dimorph II. The angles ($^\circ$) between the catechol rings and the plane of the guest molecule are 3.83 and 5.92 for dimorph I and 4.13 and 6.05 for dimorph II. The red double-headed arrow in A and C shows the 4-position ethyleneoxy arm of cryptand **12** of both dimorphs that is too far away to directly interact with **3b**; this arm is holding a water molecule. The red spheres show the oxygen atom of the water [dimorph I: $\text{O}\cdots\text{O}$ distances (Å) 2.891 and 2.923; $\text{O}\cdots\text{O}\cdots\text{O}$ angle 110.9°; dimorph II: $\text{O}\cdots\text{O}$ distances (Å) 2.838 and 2.860; $\text{O}\cdots\text{O}\cdots\text{O}$ angle 105.9°] which is closely interacting with two H_β s of **3b** [dimorph I: $\text{C}\cdots\text{O}$ distances (Å) and $\text{C}-\text{H}\cdots\text{O}$ angles ($^\circ$): 3.306, 173.1 and 3.416, 178.6; dimorph II: $\text{C}\cdots\text{O}$ distances (Å) and $\text{C}-\text{H}\cdots\text{O}$ angles ($^\circ$): 3.286, 168.5 and 3.186, 174.8].

the association constant was estimated via ^1H NMR-based competitive complexation to be $5.0 \times 10^6 \text{ M}^{-1}$ (22 $^\circ\text{C}$, acetone- d_6).^{6b} In order to standardize our methods we retested this system using ITC and found $K_a = 1.6(\pm 0.6) \times 10^6 \text{ M}^{-1}$ and $\Delta H = 15(\pm 1) \text{ kcal/mol}$ (acetone, 25 $^\circ\text{C}$).

Conclusions

In conclusion, a high yielding, regiospecific synthesis of *cis*(4,4′)-di(carbomethoxybenzo)-30-crown-10 (**1c**) was reported. The diester crown ether was converted via the diol **1d** to the pyridyl cryptand **12**, which binds paraquats (**3**) well ($K_a \geq 10^5 \text{ M}^{-1}$) and diquat (**4**) better than any other host reported to date ($K_a = 1.9 \times 10^6 \text{ M}^{-1}$) in acetone. The complexation of dibenzo-30-crown-10-based cryptand **12** with diquat **4** is at least as strong as bis(*m*-phenylene)-32-crown-10-derived cryptand **8** with paraquat **3b**, but the synthesis of the 30-crown precursor **1c** is much less time-consuming and higher yielding than synthesis of the 32-crown precursor **5a**. The 1:1 nature of the complexes of new cryptand **12** with paraquats and diquats (**3** and **4**) was

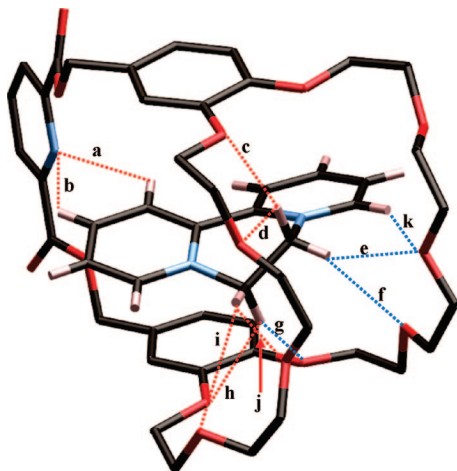


FIGURE 6. X-ray crystal structure of **12·4**. The PF_6^- counterions and hydrogens of **12** were omitted. The PF_6^- counterions are disordered. C—H...O(N) distances (Å) and angles (°) for H-bonds: **a** 3.712, 125.3; **b** 3.668, 128.81; **c** 3.240, 166.8; **d** 3.288, 112.9; **e** 3.314, 152.7; **f** 3.461, 121.4; **g** 3.355, 152.3; **h** 3.175, 129.1; **i** 3.289, 129.4; **j** 3.094, 135.2; **k** 3.257, 147.3. Both of the ester sp^3 -oxygen atoms of host **12** have weak interactions with H_6 of **4**; the C...O distances (Å) and angles (°) are 3.510, 98.0 and 3.358, 105.0. The catechol rings of **12** are stacked and the centroid-centroid distance is 7.019 Å. The distances (Å) between the catechol centroids and the plane of the guest molecule are 3.442 and 3.501. The angles (°) between the catechol rings and the plane of the guest molecule are 5.05 and 11.53.

confirmed by MS, ITC fittings, CPK modeling, and solid state structures. As other groups have improved the synthesis of functional 2,2'-bipyridines, the synthesis of derivatives of diquat **4** will lead to supramolecular polymers based on their molecular recognition by appropriate derivatives of host **12**. We are currently exploring the synthesis of cryptands based on the derivatives of the regioisomers of di(carbomethoxybenzo)-27-crown-9 as further improved hosts for paraquat guests. With synthetically available hosts with high association constants with paraquats and diquats in hand we will be able to produce true supramolecular polymers ($\text{DP} \geq 100$).

Experimental Section

Tetra(ethylene glycol) Bis(2-benzyloxy-5-carbomethoxyphenyl) Ether (10). A solution of phenol **9^{se}** (22.49 g, 87.07 mmol), K_2CO_3 (24.80 g, 179.3 mmol) and tetra(ethylene glycol) ditosylate²⁴ (22.01 g, 43.79 mmol) in CH_3CN (400 mL) was stirred at reflux for 12 h. The solids were filtered and solvent was removed *in vacuo*; the residue was partitioned between water and ethyl acetate. The water layer was extracted with ethyl acetate (3×). The combined ethyl acetate solution was washed with water and saturated NaCl solution, and dried over anhydrous Na_2SO_4 . After concentration *in vacuo*, the material was purified via column chromatography (silica/1:1 ethyl acetate:hexanes). A white solid was obtained, 27.34 g (93%), mp 68.7–69.3 °C. ^1H NMR (CDCl_3 , 400 MHz) δ 7.62 (dd, $^4J_{\text{HH}} = 2$ Hz, $^3J_{\text{HH}} = 8$ Hz, 2H), 7.57 (d, $^4J_{\text{HH}} = 2$ Hz, 2H), 7.35 (m, 10H), 6.90 (d, $^3J_{\text{HH}} = 8$ Hz, 2H), 5.17 (s, 4H), 4.21 (t, $^3J_{\text{HH}} = 5$ Hz, 4H), 3.87 (m, 10H), 3.72 (m, 4H), 3.61 (m, 4H). LR FAB MS (NBA) of **10**: m/z 558, 45% [**10** – 2 COOCH_3] $^+$; 559, 13% [**10** – 2 COOCH_3 + 1] $^+$; 560, 2% [**10** – 2 COOCH_3 + 2] $^+$; 584, 40% [**10** – $\text{C}_6\text{H}_5\text{CH}_2$] $^+$; 585, 19% [**10** + H – $\text{C}_6\text{H}_5\text{CH}_2$] $^+$; 586, 6% [**10** + H – $\text{C}_6\text{H}_5\text{CH}_2$ + 1] $^+$; 589, 26% [**10** + Li – $\text{C}_6\text{H}_5\text{CH}_3$] $^+$; 590, 9% [**10** + Li – $\text{C}_6\text{H}_5\text{CH}_3$ + 1] $^+$; 611, 9% [**10** – OCH_3 –

CH_3OH] $^+$; 612.2, 55% [**10** + H – OCH_3 – CH_3OH] $^+$; 613, 21% [**10** + H – OCH_3 – CH_3OH + 1] $^+$; 614, 6% [**10** + H – OCH_3 – CH_3OH + 2] $^+$; 643.2, 15% [**10** – OCH_3] $^+$; 644.2, 100% [**10** + H – OCH_3] $^+$; 645, 36% [**10** + H – OCH_3 + 1] $^+$; 646, 8% [**10** + H – OCH_3 + 2] $^+$; 674.3, 5% [**10**] $^+$; 675.3, 40% [**10** + H] $^+$; 676, 23% [**10** + H + 1] $^+$; 677, 8% [**10** + H + 2] $^+$. HR FAB MS (NBA/PEG): m/z 674.2712 [**10**] $^+$, calcd for $\text{C}_{38}\text{H}_{42}\text{O}_{11}$ 674.2727, error 2.3 ppm.

Tetra(ethylene glycol) Bis(2-hydroxy-5-carbomethoxyphenyl) Ether (11). To a solution of dibenzyl ether **10** (13.50 g, 20.00 mmol) in CH_2Cl_2 (100 mL) was added 10% Pd/C (0.20 g). The suspension was shaken under H_2 atmosphere (50 psi) at rt. After 12 h, TLC showed complete conversion to product. The catalyst was removed by filtration. The filtrate was concentrated to give a white solid, 9.81 g (99%), mp 60.8–62.3 °C; ^1H NMR (CDCl_3 , 400 MHz) δ 8.24 (br s, 2H), 7.62 (dd, $^4J_{\text{HH}} = 2$ Hz, $^3J_{\text{HH}} = 8$ Hz, 2H), 7.53 (d, $^4J_{\text{HH}} = 2$ Hz, 2H), 6.90 (d, $^3J_{\text{HH}} = 8$ Hz, 2H), 4.30 (m, 4H), 3.86 (m, 10H), 3.70 (m, 8H). LR FAB MS (NBA) of **11**: m/z 463, 11% [**11** – OCH_3] $^+$; 464, 100% [**11** + H – OCH_3] $^+$; 465, 25% [**11** + H – OCH_3 + 1] $^+$; 466, 5% [**11** + H – OCH_3 + 2] $^+$; 468, 33% [**11** + H + Na – H_2O – CH_3OH] $^+$; 469, 10% [**11** + H + Na – H_2O – CH_3OH + 1] $^+$; 470, 4% [**11** + H + Na – H_2O – CH_3OH + 2] $^+$; 495, 20% [**11** + H] $^+$; 496, 33% [**11** + H + 1] $^+$; 497, 10% [**11** + H + 2] $^+$; 499, 10% [**11** + Na – H_2O] $^+$; 500, 12% [**11** + Na – H_2O + 1] $^+$; 501, 4% [**11** + Na – H_2O + 2] $^+$; 518, 4% [**11** + H + Na] $^+$. HR FAB MS (NBA/PEG): m/z 494.1748 [**11**] $^+$, calcd for $\text{C}_{24}\text{H}_{30}\text{O}_{11}$ 494.1788, error 8.1 ppm.

cis(4,4′)-Di(carbomethoxybenzo)-30-crown-10 (1c). Bisphenol **11** (16.80 g, 33.97 mmol) and tetra(ethylene glycol) ditosylate (17.07 g, 33.96 mmol) were dissolved in CH_3CN (600 mL). KPF_6 (6.75 g, 36.6 mmol) and K_2CO_3 (23.80 g, 172.1 mmol) were added to the solution. The refluxing mixture was stirred under N_2 for 16 h. After cooling, the mixture was filtered and the solvent was evaporated. The material was partitioned between chloroform and water; the organic phase was washed with water, NaCl (sat. aq.), dried with sodium sulfate, filtered, and the solvent was removed. Column chromatography (neutral alumina, 1/1 v/v CHCl_3 /hexanes) yielded a white solid (20.61 g, 93%), mp 110.8–111.4 °C. We believe the melting point Huang et al.¹³ report for **1c** (149–150 °C) is likely that of the potassium salt complex with **1c**. ^1H NMR (CDCl_3 , 400 MHz) δ : 7.63 (dd, $^3J_{\text{HH}} = 8$ Hz, $^4J_{\text{HH}} = 2$ Hz, 2H), 7.52 (d, $^4J_{\text{HH}} = 2$ Hz, 2H), 6.85 (d, $^3J_{\text{HH}} = 8$ Hz, 2H), 4.18 (m, 8H), 3.88 (m, 14H), 3.78 (m, 8 H), 3.69 (m, 8H). LR FAB MS (NBA/PEG) of crude **1c**: m/z 691.7, 100% [**1c** + K] $^+$; 692.7, 35% [**1c** + K + 1] $^+$; 693.7, 17% [**1c** + K + 2] $^+$; 694.7, 4% [**1c** + K + 3] $^+$. HR FAB MS of crude **1c** (NBA/PEG): m/z 691.2352 [**1c** + K] $^+$, calc. for $\text{C}_{32}\text{H}_{44}\text{O}_{14}\text{K}$ 691.2368, error 2.3 ppm. LR FAB MS (NBA) of **1c**: m/z 622, 100% [**1c** + H – OCH_3] $^+$; 623, 34% [**1c** + H – OCH_3 + 1] $^+$; 624, 13% [**1c** + H – OCH_3 + 2] $^+$; 653, 55% [**1c**] $^+$; 654, 68% [**1c** + H] $^+$; 655, 21% [**1c** + H + 1] $^+$; 672, 81% [**1c** + H + H_2O] $^+$; 673, 28% [**1c** + H + H_2O + 1] $^+$. HR FAB MS (NBA/PEG): m/z 652.2701 [**1c**] $^+$, calcd for $\text{C}_{32}\text{H}_{44}\text{O}_{14}$ 652.2731, error 4.6 ppm.

cis(4,4′)-Di(hydroxymethylbenzo)-30-crown-10 (1d). Diester **1c** (4.00 g, 6.12 mmol) was dissolved in THF (200 mL, distilled from Na). LiAlH_4 (0.46 g, 12 mmol) was slowly added over 1 h. The mixture was stirred for an additional 12 h and then worked up using the Fieser and Fieser method.²⁵ **1d** was isolated as a white solid (3.43 g, 94%), mp 89.7–92.0 °C (lit. mp 91–94 °C^{4a}). ^1H NMR (CDCl_3 , 400 MHz) δ : 6.92 (s, 2H), 6.85 (m, 4H), 4.57 (s, 4H), 4.13 (m, 8H), 3.87 (m, 8H), 3.67 (m, 16H). LR FAB MS (NBA) of **1d**: m/z 580.24, 94% [**1d** + H – OH] $^+$; 581.2, 14% [**1d** + H – OH + 1] $^+$; 597.3, 100% [**1d** + H] $^+$; 598.3, 13% [**1d** + H + 1] $^+$; 620, 31% [**1d** + Na] $^+$; 621, 10% [**1d** + Na + 1] $^+$. HR FAB MS (NBA/PEG): m/z 596.2848 [**1d**] $^+$, calcd for $\text{C}_{30}\text{H}_{44}\text{O}_{12}$ 596.2833, error 2.5 ppm.

(24) Ouchi, M.; Inoue, Y.; Kanzaki, T.; Hakushi, T. *J. Org. Chem.* **1984**, 49, 1408–1412.

(25) Fieser, M.; Fieser, L.; Smith, J. G. *Reagents for Organic Synthesis*; Wiley: New York, 1967.

Cryptand 12. To a solution of pyridine (2.0 mL) in CH_2Cl_2 (2.5 L) were added crown ether diol **1d** (3.47 g, 5.82 mmol) in CHCl_3 (40 mL) and pyridine-2,6-dicarbonyl chloride (1.18 g, 5.78 mmol) in CHCl_3 (40 mL) simultaneously with two separate syringes via a syringe pump at 0.50 mL/h. After addition, the reaction mixture was stirred at rt 5 days. The solvent was evaporated. The crude product was redissolved in CHCl_3 and washed with 10% H_2SO_4 , water, dried with Na_2SO_4 , filtered, and concentrated via rotary evaporation. The residue was subjected to neutral alumina column chromatography, eluting with 1% MeOH in CHCl_3 . **12** was isolated as a white solid (1.86 g, 44%), mp 160.9–162.7 °C; ^1H NMR (CDCl_3 , 400 MHz): δ 8.34 (d, $^3J_{\text{HH}} = 8.0$ Hz, 2 H), 8.03 (t, $^3J_{\text{HH}} = 8.0$ Hz, 1H), 6.95 (m, 4H), 6.78 (d, $^3J_{\text{HH}} = 8.8$ Hz, 2H), 5.34 (s, 4H), 4.17 (m, 4H), 4.01 (m, 4H), 3.93 (m, 4H), 3.81 (m, 4H), 3.75 (m, 4H), 3.70 (m, 8H), and 3.64 (m, 4H). LR FAB MS (NBA) of crude **12** (before chromatography): m/z 561, 16% [**1d** – H_2O – OH or **12** – $\text{C}_7\text{H}_5\text{NO}_4$] $^+$; 562, 63% [**1d** + H – H_2O – OH or **12** + H – $\text{C}_7\text{H}_5\text{NO}_4$] $^+$; 563, 35% [**1d** + H – H_2O – OH + 1 or **12** + H – $\text{C}_7\text{H}_5\text{NO}_4$ + 1] $^+$; 564, 12% [**1d** + H – H_2O – OH + 2 or **12** + H – $\text{C}_7\text{H}_5\text{NO}_4$ + 2] $^+$; 728, 65% [**12**] $^+$; 729, 100% [**12** + H] $^+$; 730, 47% [**12** + H + 1] $^+$; 731, 14% [**12** + H + 2] $^+$; 808, 93% [**12** + $\text{C}_5\text{H}_5\text{NH}$] $^+$; 809, 42% [**12** + $\text{C}_5\text{H}_5\text{NH}$ + 1] $^+$; 810, 16% [**12** + $\text{C}_5\text{H}_5\text{NH}$ + 2] $^+$; LR FAB MS (NBA) of purified **12**: m/z 728, 73% [**12**] $^+$; 729, 100% [**12** + H] $^+$; 730, 40% [**12** + H + 1] $^+$; 731, 13% [**12** + H + 2] $^+$; HR FAB MS (NBA/PEG): m/z 727.2874 [**12**] $^+$, calcd for $\text{C}_{37}\text{H}_{45}\text{NO}_{14}$ 727.2840, error 4.7 ppm.

FAB MS Determination of the Complex 12•3a. HR FAB MS (NBA/PEG): m/z 1118.3832 [**12•3a** – PF_6] $^+$, calc. for $\text{C}_{37}\text{H}_{45}\text{NO}_{14}\bullet\text{C}_{14}\text{H}_{18}\text{O}_2\text{N}_2\text{PF}_6$, 1118.3850, error 1.6 ppm.

FAB MS Determination of the Complex 12•3b. HR FAB MS (NBA/PEG): m/z 1058.3671 [**12•3b** – PF_6] $^+$, calc. for $\text{C}_{37}\text{H}_{45}\text{NO}_{14}\bullet\text{C}_{12}\text{H}_{14}\text{N}_2\text{PF}_6$, 1058.3639, error 3.0 ppm.

FAB MS Determination of the Complex 12•4. HR FAB MS (NBA/PEG): m/z 1056.3531 [**12•4** – PF_6] $^+$, calc. for $\text{C}_{37}\text{H}_{45}\text{NO}_{14}\bullet\text{C}_{12}\text{H}_{12}\text{N}_2\text{PF}_6$, 1056.3482, error 4.6 ppm.

Example of ITC Titration Methods. Stock solutions of **12** (0.53 mM, 10 mL) and the titrant **3a** (13.8 mM, 5 mL) in acetone were prepared using volumetric glassware. All titrations were run at 22 °C. The high gain (high sensitivity) system was used, and the reference offset was set at 50% of the maximum. During each titration, 33 injections of 3.3 μL were made. Injections were made every 180 s with a primary filter period of 2 s, and a secondary filter period of 4 s. The switch time for the filter periods was at 120 s. After the titration isotherm was recorded, the raw data were reduced using commercial software and the supplied algorithms from the manufacturer. A control titration was also completed so that the heat of dilution from the titrant could be subtracted from the original titration isotherm. The parameters for the control titration were the same as those used in the original titration with the exception that the cell solution was replaced with pure acetone. The control isotherm was integrated using the same method as the original titration and the energy values obtained were subtracted from the integrated point plot of the original titration. The integration data from the titrations were fit using the “One Set of Sites” model; other stoichiometries yielded unsatisfactory fits of the data.

Acknowledgment. We acknowledge financial support of this research by the National Science Foundation through generous grants DMR0097126 and DMR0704076.

Supporting Information Available: Characterizations for all compounds and complexes (NMR, MS, ITC, 1D NOESY, and X-ray diffraction data). This material is available free of charge via the Internet at <http://pubs.acs.org>.

JO801886X